The Journal of Experimental Biology 215, 3786-3798

doi:10.1242/jeb.071092

RESEARCH ARTICLE

Keeping momentum with a mouthful of water: behavior and kinematics of humpback whale lunge feeding

Malene Simon[1,2,*], Mark Johnson[1,3] and Peter T. Madsen[1,4]

[1]Zoophysiology, Department of Bioscience, Aarhus University, C. F. Møllers Allé, Building 1131, 8000 Aarhus C, Denmark, [2]Greenland Climate Research Centre, Greenland Institute of Natural Resources, P.O. Box 570, Kivioq 2, 3900 Nuuk, Greenland, [3]Sea Mammal Research Unit, University of St Andrews, Fife KY16 8LB, UK and [4]Woods Hole Oceanographic Institution, Woods Hole, MA 02543, USA

*Author for correspondence (masi@natur.gl)

SUMMARY

Rorqual baleen whales lunge feed by engulfment of tons of prey-laden water in a large and expandable buccal pouch. According to prior interpretations, feeding rorquals are brought to a near-halt at the end of each lunge by drag forces primarily generated by the open mouth. Accelerating the body from a standstill is energetically costly and is purported to be the key factor determining oxygen consumption in lunge-feeding rorquals, explaining the shorter dive times than expected given their sizes. Here, we use multi-sensor archival tags (DTAGs) sampling at high rates in a fine-scale kinematic study of lunge feeding to examine the sequence of events within lunges and how energy may be expended and conserved in the process of prey capture. Analysis of 479 lunges from five humpback whales reveals that the whales accelerate as they acquire prey, opening their gape in synchrony with strong fluke strokes. The high forward speed (mean depth rate: 2.0±0.32 m s^{-1}) during engulfment serves both to corral active prey and to expand the ventral margin of the buccal pouch and so maximize the engulfed water volume. Deceleration begins after mouth opening when the pouch nears full expansion and momentum starts to be transferred to the engulfed water. Lunge-feeding humpback whales time fluke strokes throughout the lunge to impart momentum to the engulfed water mass and so avoid a near or complete stop, but instead continue to glide at ~1–1.5 m s^{-1} after the lunge has ended. Subsequent filtration and prey handling appear to take an average of 46 s and are performed in parallel with re-positioning for the next lunge.

Key words: baleen whale, *Megaptera novaeangliae*, gulp feeding, prey capture, dive behavior.

Received 13 February 2012; Accepted 20 July 2012

INTRODUCTION

Air-breathing marine animals display physiological and behavioral adaptations to a life in water where two vital resources are separated in space: oxygen at the surface and food at depth (Kramer, 1988). To increase time at foraging depth, breath-hold divers employ a range of oxygen-conserving measures, including a fluke and glide gait that reduces the cost of transport and hence the consumption rate of oxygen (Williams et al., 2000; Watanuki et al., 2003). Rorqual whales, a group to which blue, fin and humpback whales belong, include the largest animals ever to have evolved. A number of advantages accrue from large body size when economizing oxygen stores in diving. Large animals have a greater oxygen carrying capacity (Hochachka and Somero, 1984; Kooyman, 1989) in relation to their metabolic rate (Kooyman et al., 1980) than do small animals, and have a lower mass-specific drag (indicated by a higher Reynolds number), favoring efficient stroke-and-glide swimming (Williams et al., 2000). Accordingly, the dive times for marine mammals generally increase with body size (Hochachka and Somero, 1984; Kooyman, 1989). However, the large rorquals seem to break this rule by performing much shorter dives than would be expected given their size (Croll et al., 2001; Acevedo-Gutiérrez et al., 2002).

Balaenids and rorquals belong to the baleen whales (Mysticeti), and are specialized in filtering prey from the water (Croll and Tershy, 2002; Werth, 2000). Their relatively short dive times have been explained by the energetic costs of countering the high drag of an open mouth when the whales feed (Croll et al., 2001; Acevedo-Gutiérrez et al., 2002). Despite the similarity in filtration apparatus, the two families of baleen whales have very different strategies for prey harvesting. Balaenids generally target slow swimming prey (copepods) using continuous ram filtration (Werth, 2004; Simon et al., 2009). Their relatively long feeding dives, compared with rorquals, seem to be enabled by extremely slow swimming speeds (<0.05 body lengths s^{-1}) while foraging (Simon et al., 2009).

Rorquals, in contrast, target more elusive prey, such as schooling fish and larger crustaceans, and must employ foraging methods that are matched to the escape speed of their prey (Croll and Tershy, 2002). The usual rorqual foraging mode is lunge feeding, in which the whale accelerates forward in a burst of energetic fluke strokes to reach a high speed prior to engulfment of a volume of prey-laden water comparable to their own body volume (Pivorunas, 1979; Lambertsen, 1983; Orton and Brodie, 1987; Goldbogen et al., 2006; Goldbogen et al., 2010). Thus, rorquals forage in discrete energetic bursts with each lunge followed by an obligate refractory period in which engulfed water is expelled through the baleen plates and prey are handled and swallowed (Jurasz and Jurasz, 1979; Lambertsen, 1983; Orton and Brodie, 1987; Werth, 2000).

Until recently, lunge feeding had only been described from surface observations (Watkins and Schevill, 1979; Jurasz and Jurasz, 1979; Orton and Brodie, 1987; Croll et al., 2001). The first field measurements of sub-surface lunge-feeding rorquals were reported

by Goldbogen et al. (Goldbogen et al., 2006; Goldbogen et al., 2008; Goldbogen et al., 2011), who used multi-sensor archival tags to log total acceleration, depth and flow noise, with the latter used as a proxy for speed. Based on these recordings, Goldbogen et al. (Goldbogen et al., 2006; Goldbogen et al., 2007; Goldbogen et al., 2010) proposed a lunge-stop model for lunge feeding in which the whale first accelerates to $>3\,m\,s^{-1}$ and then opens its jaws, initiating a rapid deceleration due to the increased drag force from a radically changed body form. This deceleration ultimately brings the whale to a near standstill at the end of the lunge, requiring additional fluke strokes for the whale to regain forward motion. The lunge cycle is then completed with a period of gliding until a new bout of stroking marks the beginning of the next lunge.

Accelerating the body from a near stop after each lunge, as required by this model, is energetically costly and is purported to be the key factor determining oxygen consumption in lunge feeding (Goldbogen et al., 2006; Goldbogen et al., 2007; Goldbogen et al., 2010). However, there are several difficulties with the lunge-stop model and the measurements on which it is based, making it uncertain precisely when key biomechanical events occur in lunges. This has repercussions for evaluating what makes a lunge costly and hence addressing the evolutionary driving forces on the development and scaling of this extreme version of bulk feeding (Goldbogen et al., 2011).

According to the lunge-stop model, whales experience high drag forces as soon as they open their mouths; yet, at this point, the buccal pouch should offer little resistance to water ingress. It is not until the pouch is partially full and the elastic walls are being expanded by water pressure that drag should become a significant factor. The model also predicts that whales close their mouths after slowing to a near halt. However, such slow speeds seem contrary to the objective of engulfing mobile prey and leave little kinetic energy for the final expansion of the buccal pouch walls to maximize the engulfed water volume. Finally, whales end the lunge with an almost complete loss of momentum that must then be re-gained by fluke strokes, a tactic that seems energetically inefficient compared with maintaining some minimum forward speed. All of these considerations suggest that the opening and closing of the mouth actually occur earlier within the lunge than predicted by the lunge-stop model.

The interpretations that have led to the lunge-stop model rely upon proxies for kinematic parameters from which the relative timing of events was judged. Although lunges represent a very small proportion of the time budget of rorqual whales, these high-energy prey acquisition moments are crucial to understanding their functional morphology. Because of the short duration of lunges, high sensor sampling rates are essential to capture the details of these movements. Ideally, we would sample the whale's velocity and the relative timing of the mouth opening and closing, but sensors for gape on wild cetaceans are not currently available, and extant speed sensors are directional and so must be calibrated *in situ* over the behaviors of interest to approximate forward speed (Blackwell et al., 1999; Shepard et al., 2008). In their studies, Goldbogen et al. (Goldbogen et al., 2006; Goldbogen et al., 2007; Goldbogen et al., 2010; Goldbogen et al., 2011) relied on the amplitude of low-frequency flow noise, recorded by the tag, as a proxy for speed whereas the mouth opening state was deduced by combining speed and stroking indications derived from tag accelerometers sampled at 1 Hz. Although care was taken to calibrate flow noise against the known descent and ascent speeds of each tagged animal, the relationship between flow noise and forward speed also depends on the body form and gait, both of which change dramatically during lunges. Moreover, the low sensor sampling rate of 1 Hz used in the Goldbogen et al. studies provides few samples to work with during the brief but crucial lunge-stop phases of a lunge. Given these limitations, the details, and therefore the energetic implications of what has aptly been coined the largest biomechanical action on earth (Brodie, 1993), remain, in our view, open to debate.

To examine the fine-scale timing and development of forces in balaenopterid lunge feeding, we applied suction-cup-attached digital acoustic recording tags (DTAGs) (Johnson and Tyack, 2003) to five humpback whales foraging in West Greenland. The tags sampled triaxial accelerometers, magnetometers and a pressure sensor at 50 Hz (5 Hz sensor bandwidth due to anti-alias filter) allowing body movements during foraging to be resolved with precision. Using this data set, we here investigate the relative timing of events within a rorqual lunge, identifying possible mouth opening and closing signatures in the acceleration signal. Based on the resulting timing model, we explore how kinetic energy is expended and conserved during lunges, showing that this prey-capture mechanism is likely more efficient and better suited to the capture of mobile prey than predicted by prior models. Finally, we show that humpback whale lunges and the refractory prey-handling period between lunges have a high degree of stereotypy, indicating that biomechanical constraints rather than prey density limit the lunging frequency. Despite the low duty cycle of lunges, we suggest that the higher density of prey targeted by lunging rorquals may enable them to acquire prey at rates similar to those of continuous filtering balaenids.

MATERIALS AND METHODS

Humpback whales (*Megaptera novaeangliae* Borowski 1781) in the Godthåbsfjord, West Greenland (64.2°N, 51.8°W), were tagged with non-invasive, archival tags (DTAGs) (Johnson and Tyack, 2003) to record data on their three-dimensional movements during lunge feeding. Humpback whales were located either from a vantage point on land or by searching the fjord with two small boats. Whales were approached slowly from a 6 m (2007) or 7 m (2008) aluminum motor boat, and the tag was attached to the dorsal surface of the whale with suction cups using a 7 m hand-held carbon fiber pole (2007) or a 12 m cantilevered carbon fiber pole (2008) (Moore et al., 2001). The suction cups detached after a pre-programmed period and were retrieved using VHF tracking.

Research was conducted under a permit granted by the Greenland Government to the Greenland Institute of Natural Resources.

DTAGs

The DTAG is an archival tag that streams sound and orientation data to a 16 GB solid-state memory using loss-less compression (Johnson and Tyack, 2003). Three-axis magnetometers and accelerometers ($\pm 2\,\boldsymbol{g}$ range) provide signals relating to the orientation and acceleration of the animal in three dimensions and a pressure sensor provides depth information. All sensors are sampled at 50 Hz with 16 bit resolution and decimated to a sampling rate of 25 Hz in post-processing. Each sensor channel has a single pole anti-alias (low-pass) filter at 5 Hz and decimation is achieved using identical 24-tap symmetric finite impulse response (FIR) filters on each channel. The accelerometer and magnetometer data were corrected for the tag orientation on the whale by rotating each three-element vector by a direction cosine matrix derived from the tag orientation when the whale surfaces (Zimmer et al., 2005). The resulting rotated vectors approximate the sensor measurements that would be made if the tag axes coincided with the body axes of the whale (Johnson and Tyack, 2003). Sounds were recorded continuously from a built-

in hydrophone with a sampling rate of 96 kHz, 16 bit resolution and a nominally flat (±2 dB) frequency response from 0.4 to 47 kHz (Johnson and Tyack, 2003).

Fluke strokes, specific acceleration and jerk

Fluke movements during cetacean swimming generate thrust and heave accelerations and cause undulations through most of the body (Fish et al., 2003), all of which contribute cyclical variations to the on-animal accelerometer signals (Johnson and Tyack, 2003; Sato et al., 2007). The relative magnitude of these components depends on the size of the animal. On large animals that stroke relatively slowly, body rotation may be the dominant indicator of stroking. However, the magnitude of this signal in each accelerometer axis depends on the animal's posture. In horizontal swimming, the rotation will be clearest in the caudal–rostral accelerometer axis, whereas during near-vertical descents and ascents, the signal is most evident in the dorso-ventral axis. To track fluking throughout dives, we first estimated the mean body posture by low-pass filtering the accelerometer and magnetometer vectors (0.15 Hz, zero-group-delay FIR filter) to remove the fluking signal. A direction cosine matrix (also known as a rotation matrix) describing the mean orientation at each time step was constructed from these smoothed signals (Johnson and Tyack, 2003). A direction cosine matrix was also formed from wider-bandwidth accelerometer and magnetometer signals (filtered with a 1 Hz, zero-group-delay FIR low-pass filter) that include fluking movements. A pitch deviation signal was produced by measuring the rotation angle in the sagittal plane between these matrices, i.e. between the mean and the instantaneous body postures, at each time step. This signal summarizes the short-term movements of the animal in a way that is consistent irrespective of the posture. The duration of each fluke stroke was then measured from the time lapse between pairs of zero crossings in the pitch deviation signal.

The acceleration signal recorded by the tag during fluking is dependent on both the orientation of the body (i.e. the gravitational acceleration component) and the specific acceleration of the animal at the tag location (i.e. the acceleration due to actual movements of the animal). Both of these acceleration components have energy at the fluking rate and cannot be separated (Johnson et al., 2009), meaning that the acceleration signal cannot be integrated to give a speed estimate. Both orientation and specific components in the measured acceleration are dependent on the location of the tag on the body and on the gait of the whale, making the magnitude of the accelerometer signal only useful as a relative (i.e. intra-individual) estimator of stroking strength. Nonetheless, energetic stroking during rorqual lunges produces distinctive accelerometer signals (Goldbogen et al., 2006) that can be used to quantify movement events within lunges. The acceleration, A, measured by the tag as a function of time, t, can be expressed as:

$$A_t = \mathbf{Q}_t\mathbf{G} + \mathbf{D}_t, \quad (1)$$

where $\mathbf{G}$ is the gravitational acceleration vector $[0,0,1]^T$ (defined here in units of $\boldsymbol{g}$, $\boldsymbol{g}$=9.81 m s^{-2}, and in a right-hand frame with axes north, west and down), $\mathbf{Q}_t$ is a direction cosine matrix defining the orientation of the tag with respect to the inertial frame as a function of time t, and $\mathbf{D}_t$ is the specific acceleration vector, also a function of t. In the absence of specific acceleration, the norm of A, defined as $\|A\|=\sqrt{(a_x^2 + a_y^2 + a_z^2)}$, will be 1 $\boldsymbol{g}$, i.e. the strength of the earth's gravitational field. If the measured norm differs from this, it is an indication that there is some specific acceleration due to movement of the animal. Although it is not possible to estimate the specific acceleration directly, a lower bound on its magnitude can be obtained from $\|A\|$ as follows. Re-arranging Eqn 1 and taking the norm of both sides gives:

$$\|\mathbf{D}_t\|^2=\|A_t\|^2 + \|\mathbf{Q}_t\mathbf{G}\|^2 - 2A_t{}^T\mathbf{Q}_t\mathbf{G}. \quad (2)$$

Applying the Schwarz inequality (Golub and Loan, 1996) gives:

$$\|\mathbf{D}\|^2 \geq \|A\|^2 + \|\mathbf{QG}\|^2 - 2\|A\|\,\|\mathbf{QG}\|. \quad (3)$$

As rotation matrices are unitary (Grewal et al., 2001), $\|\mathbf{QG}\|=\|\mathbf{G}\|=1\,\boldsymbol{g}$. So Eqn 2 becomes:

$$\|\mathbf{D}\|^2 \geq \|A\|^2 - 2\|A\| + 1$$
$$\text{or } \|\mathbf{D}\| \geq |\,\|A\| - 1|. \quad (4)$$

Thus, the magnitude of the specific acceleration in units of $\boldsymbol{g}$ is bounded below by the absolute value of $\|A\|$–1, which can be readily calculated from the measured acceleration signals. We call this quantity the minimum specific acceleration (MSA).

Another useful quantity relating to the changing forces produced and experienced by the whale is the acceleration rate of change, coined 'jerk'. Jerk can be estimated by differentiating (or, for sampled data, differencing) the triaxial acceleration signal and is a useful indicator of fast movements or changes in orientation. To combine this vectorial signal into a more easily visualized scalar, we computed the norm of the jerk, i.e. $j_t=\|A_t–A_{t–T}\|/T$, where T is the sensor sampling period. Being computed from the same sensor data, jerk is inherently related to MSA but provides a different view of the underlying movements. Thus, steady stroking will give rise to cyclic variations in MSA and j_t at twice the stroking rate because acceleration both peaks twice (in absolute value) and changes rapidly twice in a fluke cycle (i.e. on each upstroke and downstroke). However, relatively small, rapidly changing forces on the whale, e.g. due to mouth opening/closing or fast maneuvers, will cause high-frequency transients in the jerk signal that may be difficult to detect in the MSA.

Lunge timing and orientation

Goldbogen et al. (Goldbogen et al., 2006) used low-frequency flow noise over the tag as a proxy for swimming speed and to detect and time lunges. They measured flow noise using a third-octave filter centered at 50 Hz and considered a peak in the flow noise equivalent to a speed >2 m s^{-1} to indicate a lunge. To time events during lunges, they defined a 'zero-time' as the time within each lunge of the peak in flow noise. The tag used here has a high-pass filter at 400 Hz precluding the exact replication of Goldbogen et al.'s method. However, a clear flow noise signal was nonetheless apparent in the sound recording and we used this to detect lunges. To do so, we first low-pass filtered the sound recording (fourth-order Butterworth filter at 500 Hz) and computed the root mean square (r.m.s.) level in 40 ms blocks to obtain a flow noise estimate with the same sampling rate (25 Hz) as the non-acoustic tag sensors. As described by Goldbogen et al. (Goldbogen et al., 2006), the acoustic signature of lunges comprises a period of strong flow noise lasting several seconds followed by a rapid reduction in noise level. These events are readily detected by eye in the flow noise profile and in other sensor signals but, to reduce subjectivity, we used an automatic detector that analyzed the r.m.s. flow noise in 1 s bins. This detector identified noise peaks that: (1) exceeded the 90th percentile of the noise level during all dives (depth >10 m) and (2) were followed by at least a 12 dB reduction in level within 5 s. Comparing the resulting detections with a subjective evaluation, we found a small number (~2%) of false detections, i.e. flow noise pulses that did not coincide with stroking, and these were eliminated. The automatic method missed ~10% of lunges that were detected subjectively, but

only the automatic detections were used for analysis. To avoid the complication of changing buoyancy and drag forces when animals lunge at the surface, we only analyzed lunges occurring deeper than 40 m (approximately three body lengths). As in Goldbogen et al. (Goldbogen et al., 2006), we also used the flow noise to define a zero-time in lunges as a reference point to compare against the signals from other sensors. Goldbogen et al. (Goldbogen et al., 2006) used the peak point of the flow noise to define the lunge zero-time; however, with the higher temporal resolution available here, we found that many lunges had several peaks in the flow noise, making this cue ambiguous. Instead, we chose the half-power end point of the flow noise envelope (i.e. the –3 dB point relative to the peak value of flow noise) during each lunge as the zero-time. This easily identified unambiguous event helped to ensure consistency in the way lunges and their timing from different animals were identified and analyzed.

The mean orientation of the whale throughout the lunge was estimated by taking the mean of the acceleration vector over the interval spanning –5 s before to +5 s after the zero-time. Samples with MSA >1 m s^{-2} were excluded to minimize the inclusion of specific acceleration in the mean. The mean pitch and roll were deduced from the resulting acceleration vector as described previously (Johnson and Tyack, 2003).

Speed estimation

The speed of marine animals has been estimated using a variety of tag-based sensors, including paddlewheels (Blackwell et al., 1999), bending filaments (Shepard et al., 2008), flow noise (Burgess et al., 1998) and orientation-corrected depth rate (Miller et al., 2004). Several sources of error impact these measurements during energetic events such as lunging. Much of the body displacement during stroking is in the dorso-ventral axis (Fish et al., 2003). As a result, the instantaneous speed of a point on the body is greater, on average, than the forward speed by an amount dependent on the stroking rate and magnitude. The magnitude of oscillations from stroking increases the closer to the fluke the tag is placed (Fish et al., 2003) and therefore the position of the tag on the body will also affect the total acceleration of the tag. Thus, speed sensors on stroking animals tend to overestimate forward speed, requiring *in situ* calibration to correct this error for each gait and placement (Blackwell et al., 1999). Lift tends to have the opposite effect. With lift, the mean axis of movement does not coincide with the mean longitudinal axis of the whale, potentially leading to underestimation of speed. Rorquals both fluke energetically and use their flippers to create lift during lunge feeding (Fish et al., 2008; Cooper et al., 2008) making both sources of error difficult to avoid. Errors cannot be easily calibrated out because they result from behavior that is unlikely to occur in calibration intervals (usually the descent or ascent in deep dives).

To work around these various error sources, we use three different proxies to investigate how speed changes during lunges, namely: (1) flow noise, (2) depth rate and (3) orientation-corrected depth rate. We used flow noise to investigate peak speed and speed loss within lunges relative to ascents and descents. For each animal, we plotted the log of flow noise (r.m.s. over 1 s bins) against depth rate during steep (>70 deg absolute pitch angle) sections of descents and ascents. This plot was then used as a calibration to interpret flow noise over 1 s bins during lunges. This likely gives an overestimate of forward speed because of the high-magnitude stroking, higher drag body form and additional noise from water entering the mouth during lunges. To qualify this measure, we used depth rate to estimate the minimum forward speed during lunges. Pressure sensors are insensitive to the high specific acceleration within lunges and, when averaged over fluke strokes, provide an accurate estimate of the vertical distance covered per unit of time. We used the mean depth rate from –5 s to +5 s relative to the lunge zero-time as a lower bound on lunge speed. Because the pitch angle is often low during lunges, we did not attempt to correct the depth rate for the orientation of the whale to improve the speed estimate (Miller et al., 2004) within lunges. The orientation-corrected depth rate, averaged over 1 s intervals, is useful, however, to quantify speed development during the 10 s immediately after each lunge where the pitch angles are consistently high. This measure is calculated from $(d_t–d_{t–T})/\sin\rho_t$, where d_t is the depth reading at time t and ρ_t is the mean pitch angle over the T=1 s interval. Specific acceleration affects the accuracy of the pitch angle estimate (Johnson and Tyack, 2003) and hence the speed estimate, with the effect being most pronounced at low pitch angles. In the 10 s at the end of lunges, the pitch angle tends to be high (>30 deg) and the MSA low due to less energetic stroking or gliding, making the orientation-corrected speed estimate reasonably reliable. Therefore, speed was not estimated in 1 s intervals with absolute mean pitch angles <30 deg, resulting in a speed error of <20% if the mean specific acceleration over the 1 s interval is <1 m s^{-2}. A similar method was used to estimate speed during descents and ascents, where the mean depth rate per second was divided by the mean low-pass filtered (0.15 Hz, zero-group-delay FIR) pitch angle for the same time interval.

RESULTS

Five humpback whales were tagged in Godthåbsfjord, Greenland, between 2 and 25 July 2007 (IDs mn180a, mn192a and mn203a) and between 25 May and 4 June 2008 (IDs mn155a and mn156a). The tags stayed on the whales for periods of 4.7–25.2 h. The three tags in 2007 were placed behind the dorsal fin to aid the acquisition of stroking patterns within lunges whereas the tags of 2008 where placed well forward (>2 m) of the dorsal fin to emphasize detection of mouth opening during lunging.

Diving behavior

A total of 164 foraging dives (defined as dives deeper than 40 m with lunges) were recorded, with maximum depths ranging from 81 to 267 m. Multi-hour feeding bouts were performed by all five whales with consecutive dives targeting the same depth layer ±20 m (Fig. 1). Whales fluked continuously within the first 30–40 m of descents, with a mean stroke rate of 0.20–0.29 Hz (Table 1). Deeper in the descent, stroking became intermittent or ceased altogether until the foraging depth was reached (Fig. 2A,B). When ascending, whales fluked steadily at 0.24–0.32 Hz until they reached a depth of 30–40 m, after which stroking became occasional or ended and the whales glided to the surface (Fig. 2A,B, Table 1). The link between stroking/gliding gaits and vertical direction suggests that these whales are denser than water once gasses carried by the whale are compressed at depth and so tend to sink unless actively swimming (Nowacek et al., 2004). The mean (±s.d.) speed (from the orientation-corrected depth rate) was uniformly high during descent (2.3±0.4 m s^{-1}) and ascent (2.1±0.3 m s^{-1}), with peak speeds reaching more than 3 m s^{-1} (Table 1).

Lunges

Tagged whales performed vertical excursions of 10 to 40 m amplitude during the bottom phase of most dives deeper than 40 m. These depth dynamics coincided with signatures of lunges following the definitions of Goldbogen et al. (Goldbogen et al., 2006) (Fig. 2). We identified 479 lunges (Table 2) using the automatic flow-noise detector. The depth of lunges was fairly constant within individuals

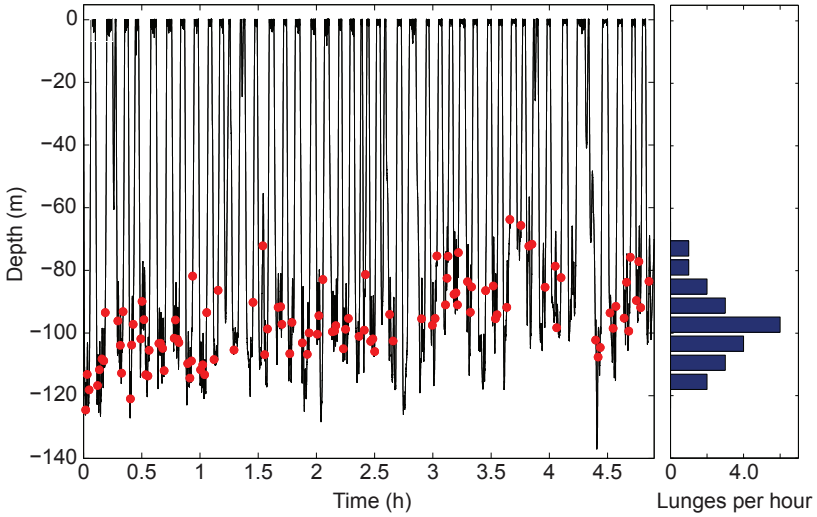

Fig. 1. Depth profile of a humpback whale tagged with a DTAG in Godthåbs Fjord, Greenland. The red circles indicate lunges and the histogram on the right summarizes the depth distribution of the number of lunges per hour (bin width: 5 m).

(Fig. 1), but varied widely with means from 54 to 236 m across animals, likely reflecting differences in the depth of the prey layer at the time of tag attachment. The lower limit of the lunge depth range is restricted by our definition of subsurface dives (40 m, chosen to avoid lunges with complex dynamics due to changing buoyancy forces and surface interactions) and does not reflect the actual minimum depth limit. One whale (mn203a) performed two separate feeding bouts, each lasting several hours and targeting different prey layers with mean depths of 84 and 171 m, suggesting that lack of intra-individual variability in other tag recordings may relate to short recording times rather than individual depth preferences.

The depth excursions during lunges showed a stereotypical dive behavior, with the large majority of lunges being performed in an ascending direction and the final lunge in many dives being performed on the ascent to the surface. To illustrate this stereotypy, the depth profiles of all lunges performed by whale mn156 are plotted in Fig. 3 relative to the depth at the zero-time of each lunge. The lunges from the other four whales show a similar stable pattern although one whale (mn203a) performed 17% of lunges during the descending or bottom part of depth excursions. Otherwise, the few lunges that did not follow the stereotypic pattern of Fig. 3 occurred at the end of the descent or at the beginning of the ascent where the whales briefly mixed transport and foraging.

The number of lunges per foraging dive ranged from 1 to 9 with a mean of 3.4±0.63 (maximum per whale of 4–9; Table 2). The mean time intervals between lunges were fairly similar across the five whales, with means ranging from 47.8 to 60.5 s. The mean pitch angle during lunges ranged from 27 to 44 deg across whales. The mean roll was consistently low in lunges (–2 to –17 deg; Table 2) and all whales except mn155a had a small left roll tendency, although this may reflect errors introduced when correcting the data for the orientation of the tag on the whale.

Lunges comprised a short burst (mean=3.0±0.61 fluke strokes, range=1–7) of increasingly fast fluke strokes accompanied by a suite of other indications of energetic movement including peaks in flow noise, MSA, jerk and depth rate (Fig. 4). The fastest fluke stroke in lunges (0.4–0.5 Hz; Table 2) was 40–110% faster than during descents or ascents (rank-sum test for increased stroking rate in lunges by individual: $P<<0.01$). Likewise, the MSA, averaged over fluke strokes, was two to seven times higher than in descents and ascents (rank sum for increased MSA within lunges: $P<<0.01$). The flow noise within lunges is comparable to, although a little higher than, the peak speeds measured in descents and ascents (Fig. 4), suggesting peak lunge speeds of 3–4 m s^{-1}. This is supported by the depth rate, a lower bound on forward speed, which has a mean of almost 2 m s^{-1} despite the low mean pitch angle. Although peaks in flow noise were used to detect lunges, leading to a bias towards high speed estimates, only some 10% of additional lunges were identified by subjective appraisal of the sensor data, suggesting that this bias is not great.

The relative timing of peaks in the speed and acceleration signals suggests that lunges can be divided into phases that may relate to the different biomechanical events taking place. During the stroking bout associated with each lunge, the speed proxies increase, a clear jerk signal appears and whales accelerate to a peak MSA with per-individual means of up to 8.8 m s^{-2} depending on the tag location

Table 1. Dive data summary for five tagged humpback whales

	mn180a	mn192a	mn203a	mn155a	mn156a
Foraging dives	10	39	49	35	31
Descent speed (m s^{-1})	3.0±0.18	2.2±0.31	2.2±0.42	2.0±0.22	2.2±0.31
Descent fluking rate (Hz)	0.29±0.08	0.24±0.02	0.20±0.02	0.24±0.04	0.29±0.10
Descent MSA during fluking (m s^{-2})	0.69±0.22	0.23±0.05	0.19±0.11	0.27±0.08	0.39±0.08
Ascent speed (m s^{-1})	2.3±0.16	2.0±0.31	2.0±0.36	1.8±0.19	2.6±0.36
Ascent fluking rate (Hz)	0.32±0.07	0.25±0.03	0.24±0.04	0.24±0.05	0.27±0.08
Ascent MSA during fluking (m s^{-2})	1.1±0.27	0.38±0.15	0.44±0.09	0.41±0.17	0.49±0.36

Foraging dives are defined as dives with lunges deeper than 40 m. Descents end at the first positive pitch angle and ascent starts at the last negative pitch angle. The speed is the mean of the pitch-angle-corrected depth rate. The fluking rates are the dominant fluking rates, not influenced by gliding periods.
MSA, minimum specific acceleration.
Data are means ± s.d.

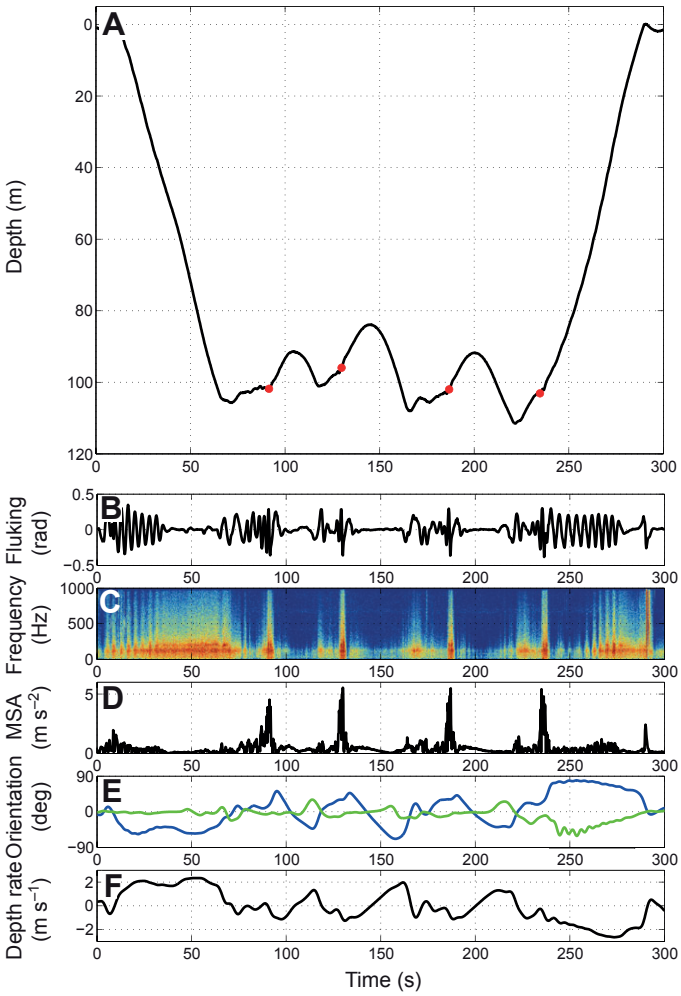

Fig. 2. A humpback foraging dive with four lunge-feeding events. (A) Depth profile, with lunges indicated by red circles. (B) Pitch deviation due to stroking movements in radians (0.15–1 Hz band-pass filter). (C) Spectrogram of the sound recording decimated to 2 kHz (FFT=512, Hann window, 50% overlap), showing increased flow noise over the tag during descent, ascent and lunge events. (D) Minimum specific acceleration (MSA), showing clear peaks during lunges. (E) Body orientation of the diving whale in degrees (blue line, pitch; green line, roll; 0.2 Hz low-pass filter). (F) Depth rate (proxy for minimum forward speed; 0.5 Hz low-pass filter).

on the animal (Fig. 4, Table 2). The MSA reaches a peak ~2 s before the lunge zero-time (Fig. 4E). Shortly thereafter (–1 s), the fluke noise and depth rate reach a peak indicating the time of maximum speed (Fig. 4D,G, Fig. 5, Table 3). The rapid drop in flow noise and depth rate that define the zero-time of lunges occur despite a relatively stable pitch angle, providing conclusive evidence for a substantial loss of speed between times –1 and 1 s. Stroking is tightly synchronized with this speed drop (Fig. 4): in all animals, the drop in flow noise occurs near the start of the upstroke of the final fluke stroke. This fluke stroke is slow and incomplete in many lunges, ending (where this can be measured) an average of 3.8 s after lunge zero-time. The jerk signal has several peaks earlier within the lunge largely synchronized with rapid stroking. However, a last transient in the jerk signal appears in most lunges at approximately second +1.3 (±0.45). This peak does not seem to be related to stroking and occurs well after the drop in flow noise (Fig. 5), suggesting that body movements other than propulsion are responsible. Thus, the high sampling rate biomechanical signals show a progression of events during lunges that can be summarized as follows. First, stroking generally starts with an upward pitch angle, leading to an increase in speed. Second, the stroking rate and MSA reach a peak. Third, forward speed, as estimated from flow noise, reaches a peak at some 3–4 m s^{-1}. Fourth, speed decreases rapidly and synchronously with the start of the final fluke stroke. Fifth, a final jerk transient occurs. And finally, the whale glides while re-positioning for the next lunge.

It has been hypothesized that rorquals come to a near halt immediately after, and as a consequence of, lunges (Goldbogen et al., 2006; Goldbogen et al., 2007). To investigate this lunge-stop hypothesis for humpback whales, we computed the pitch and speed in 1 Hz bins from the lunge zero-time to 10 s after the lunge. The whale's forward speed was estimated by taking the mean of the orientation-corrected depth rate over 1 s bins (Fig. 6). During the 10 s after the lunge, the pitch was uniformly high (>30 deg) and fluke strokes stopped completely within the first 4 s, making this speed estimate fairly reliable. Fig. 6 shows that the whales did not come to a halt, but rather kept gliding at a constant speed just above 1 m s^{-1}. The further away from the head the tag was attached, the larger the specific acceleration experienced from stroking (Fish et al., 2003). Thus, tags on whales mn180 and mn203, which were closer to the flukes than on the other whales, recorded more variable speed estimates during the first 2 s after the lunge (zero-time) (Fig. 6C), becoming more consistent when stroking ended.

DISCUSSION

The energetic cost of lunge feeding is believed to explain the short dive times of rorquals (Croll et al., 2001; Acevedo-Gutiérrez et al., 2002). But, although our understanding of rorqual foraging has increased recently thanks to technological advances (Goldbogen et

Table 2. Summary of lunge data in deep (>40 m) dives

	mn180a	mn192a	mn203a	mn155a	mn156a	Mean
Number of lunges	53	110	155	86	75	
Lunges per dive	2.9±1.71	2.9±1.24	4.4±1.75	3.5±1.32	3.1±1.61	3.4±0.63
Inter-lunge interval (s)	60.5±40.69	58.3±27.12	57.6±23.60	47.8±16.60	58.2±38.04	56.5±4.98
Mean pitch in lunge (deg)	33.3±27.84	36.8±9.84	27.6±14.62	37.6±12.36	44.1±16.63	35.9±6.05
Mean roll in lunge (deg)	–12.0±15.69	–6.5±5.81	–13.4±7.55	–1.8±22.62	–16.5±17.09	–10.0±5.86
Mean depth rate (m s^{-1})	1.8±0.64	1.6±0.47	2.4±0.93	2.1±0.41	2.2±0.51	2.0±0.32
Flukes per lunge	2.4±0.61	2.4±1.06	2.8±1.04	3.5±1.07	3.7±1.13	3.0±0.61
Max fluking frequency (Hz)	0.45±0.10	0.52±0.10	0.47±0.12	0.41±0.09	0.42±0.09	0.45±0.05
Peak of MSA (m s^{-2})	8.8±3.50	8.7±1.60	5.2±1.53	3.6±0.88	3.2±0.61	5.9±2.71
Mean MSA over fluke stroke (m s^{-2})	3.3±1.3	2.6±1.0	2.1±0.8	1.1±0.3	1.0±0.3	2.0±0.98

Means (±s.d.) of each parameter are given.
MSA, minimum specific acceleration.

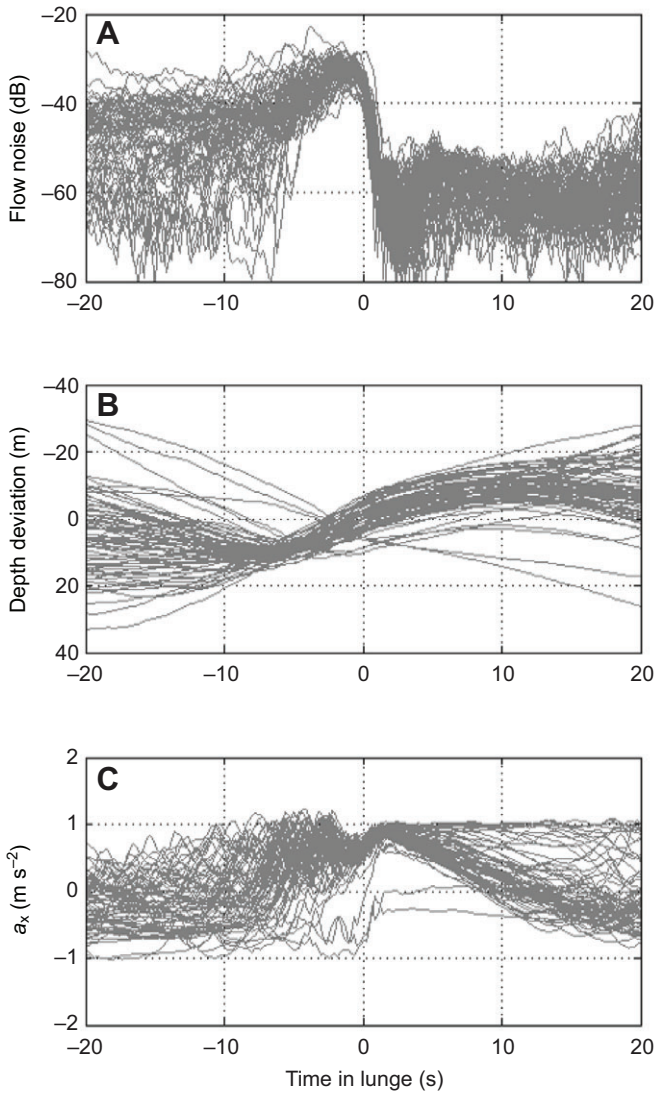

Fig. 3. Flow noise, depth and acceleration during lunges performed by whale mn156a, showing the high degree of stereotypy. (A) Low-frequency noise amplitude in dB. (B) Depth, smoothed with a 4 Hz low-pass filter, during lunges. The mean depth in each lunge over the 40 s window has been removed. (C) Total acceleration in the *x*-direction (i.e. caudal–rostral), smoothed with a 4 Hz low-pass filter. This signal represents both the body pitch angle and the forward acceleration from stroking.

al., 2006; Goldbogen et al., 2008; Goldbogen et al., 2011; Calambokidis et al., 2007; Ware et al., 2011; Doniol-Valcroze et al., 2011), the details of how lunges are performed at depth are largely based on inferences from low-resolution sensor data (Goldbogen et al., 2006). Here we use fast-sampling multi-sensor tags to provide a higher-resolution picture of the kinematics and behavior of rorqual lunge feeding. Our results suggest that the biomechanical events taking place within lunges occur in a slightly different sequence from that predicted by the current lunge-stop model of Goldbogen and coworkers. Given the energy involved in lunge feeding and the importance of this mode of prey acquisition for rorquals, these small timing differences may make a large difference in the way we evaluate the foraging energetics of these marine predators and the evolutionary forces that led to the anatomical and eco-physiological specializations that support this foraging style.

The U-shaped foraging dives performed by tagged humpback whales in the present study are similar to those reported previously for blue, fin and humpback whales (Croll et al., 2001; Goldbogen et al., 2006; Goldbogen et al., 2008; Goldbogen et al., 2011; Ware et al., 2011), comprising a steep descent to the foraging depth, a number of descending–ascending excursions associated with lunges, followed by a steep ascent to the surface. The fluke-and-glide behavior during descents and ascents suggests that whales in this study had a body density greater than water (Fig. 2). This means that whales will tend to sink below the depth of lung collapse unless they are actively swimming, a result also in accordance with earlier studies (Goldbogen et al., 2006; Goldbogen et al., 2008; Williams et al., 2000). However, when it comes to the details of the behavior, kinematics and energetics of how rorquals execute a lunge, our high-resolution data offer some significant new insights. Following the Nyquist sampling theorem, a sampling rate of at least two times the maximum frequency of a signal is needed to avoid aliasing and the resulting ambiguity in timing and frequency estimation. In practice, the sampling rate should be more than three times the highest frequency of interest to allow for anti-alias filtering. Here we show that humpback whales can fluke at 0.5 Hz during lunges (Table 2). These data come from sensors sampled at 50 Hz with 5 Hz anti-alias filters (one pole) and so are free from aliasing. Goldbogen et al. (Goldbogen et al., 2006) used tags sampling at 1 Hz and found a mean stroke rate of 0.27 Hz during fin whale lunges. No anti-alias filters were specified and it is uncertain whether these stroking rates are affected by aliasing. Regardless of whether this is the case, 1 Hz data provide little resolution of the transient accelerations that may occur during lunges, making it difficult to distinguish biomechanical events. Thus, even for large animals, high sampling rates and adequate anti-alias filtering are needed when acquiring on-animal sensor signals if the details of dynamic foraging events are of interest.

A significant problem facing biomechanical studies of foraging in cetaceans is a lack of sensors for the specific parameters of interest, namely vectorial speed and gape. Instead, these parameters must be inferred from other sensors using knowledge of biomechanics and sensor limitations to resolve ambiguities. Goldbogen et al. (Goldbogen et al., 2006; Goldbogen et al., 2007) used flow noise over the tag as an estimate of speed to argue that fin whales first accelerate to some 3 m s^{-1} during lunges but then decelerate sharply to a near halt. They associated the deceleration with the increased drag of an open mouth and deduced that the mouth opening must happen when the flow noise (and hence inferred speed) starts to drop. We observed the same overall pattern of flow noise in on-animal sound recordings from lunge-feeding humpback whales (Figs 1, 2, 4). However, analysis of our fine-scale accelerometer and depth data suggests a different interpretation of this signal. In the following, we will discuss the details of humpback lunge feeding as revealed by these data and address implications for the existing models for rorqual feeding behavior and kinematics (Goldbogen et al., 2009; Goldbogen et al., 2010; Potvin et al., 2009; Potvin et al., 2010).

Lunges

Tagged humpback whales produced approximately three strong fluke strokes during lunges, accelerating to reach a maximum speed of 3–4 m s^{-1}. This speed was then shed abruptly, creating a sharp falling edge in the flow-noise signal. Thus whales finish lunges with a much-reduced forward speed but the precise speed is difficult to deduce from the flow noise because of the high variability of this proxy at low speeds (Fig. 5). Fortunately, whales in our data exited most lunges gliding with an upward pitch angle, making the

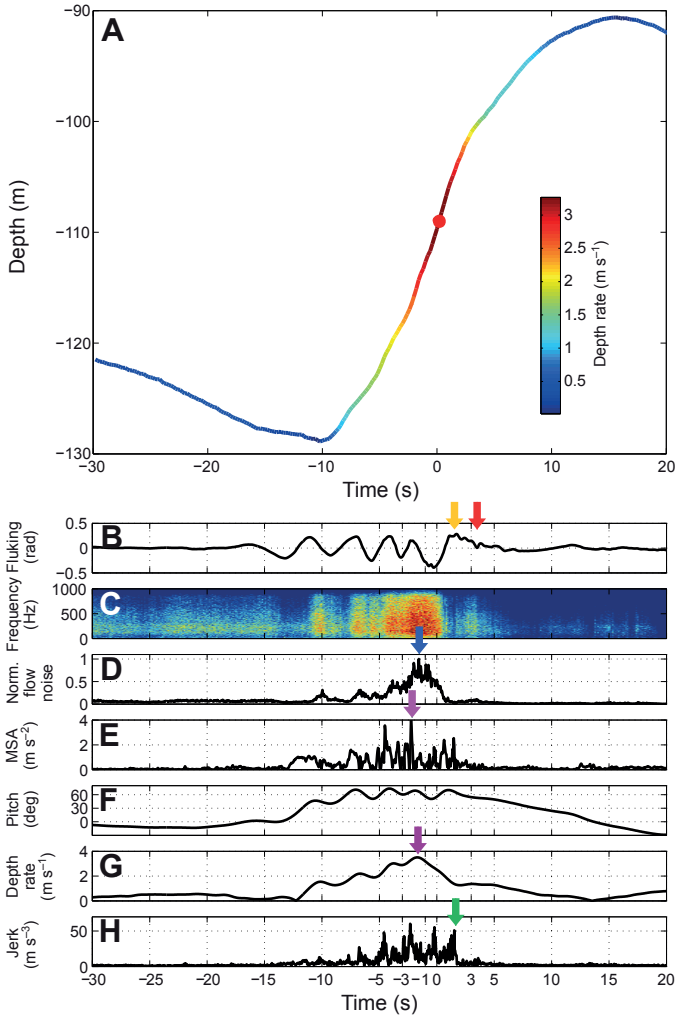

Fig. 4. Detailed study of a single lunge. (A) Depth profile (colors indicate depth rate). (B) Pitch deviation in radians showing fluke strokes (0.15 Hz high-pass filter). (C) Spectrogram of sound recording decimated to 2 kHz (FFT=512, Hann window, 50% overlap). (D) Normalized flow noise. (E) Minimum specific acceleration (MSA). (F) Pitch angle in degrees (0.5 Hz low-pass filter). (G) Depth rate (0.5 Hz low-pass filter). (H) Jerk (magnitude of the differential of triaxial acceleration).

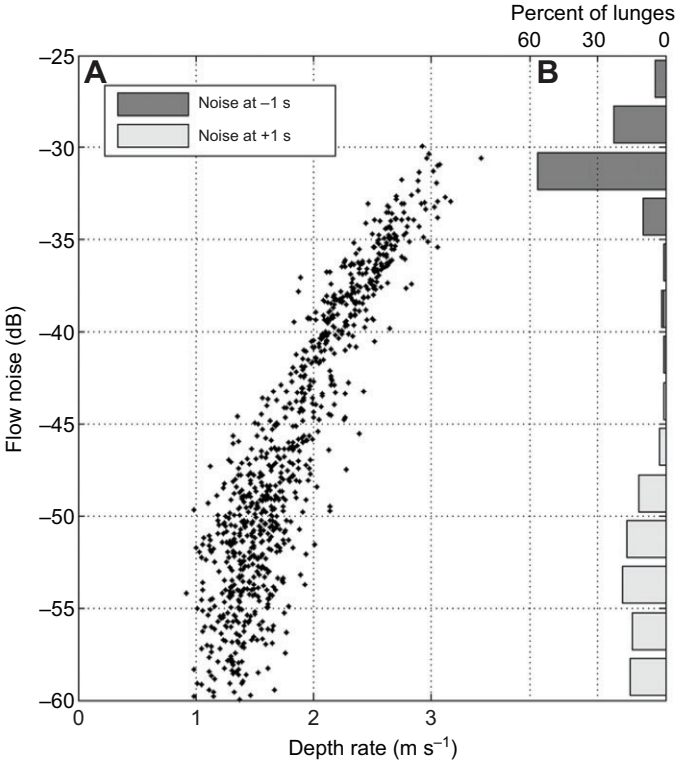

Fig. 5. (A) Relationship between depth rate and flow noise (1 s r.m.s.) during high-pitch-angle descents and ascents for whales mn155a and mn192a. (B) The histograms show the flow noise measured during lunges 1 s before (dark grey) and 1 s after (light gray) the flow-noise drop that defines the lunge zero-time. The peak flow noise indicates a maximum speed in lunges of some 3–4 m s^{-1}.

orientation-corrected depth rate a reliable proxy for speed. Using this measure, we found that whales finished lunges with a consistent forward speed of 1–1.5 m s^{-1} (Fig. 6). Moreover, this speed was maintained while gliding, showing that by the end of the lunge, whales have transferred momentum to the acquired water mass and do not require additional thrust to maintain forward motion.

From a conservation of momentum viewpoint, the rough halving in speed from a peak of 3–4 m s^{-1} to an ending speed of 1–1.5 m s^{-1} is consistent with a transfer of momentum to an engulfed water volume equal to the body mass of the whale, a volume also predicted by anatomy and observation (Goldbogen et al., 2010). That humpback whales end lunges with a speed of ~1–1.5 m s^{-1} is also supported by two other studies using pressure change (Ware et al., 2011) and flow noise (Goldbogen et al., 2008) as speed proxies (see Fig. 4). However, this momentum-sharing behavior is at odds with the near-halts inferred in fin whale lunging by Goldbogen et al. (Goldbogen et al., 2006; Goldbogen et al., 2010). Fin whales exhibit positive allometry of the skull and buccal pouch, which may result in relatively larger drag during lunges for larger whales (Goldbogen et al., 2010; Goldbogen et al., 2012). If this also holds across rorqual species it could explain the apparent differences in speed at the end of lunges in fin whales (body length 25 m) and humpbacks (15 m). However, that would still leave the question of why these large filter feeders should bring themselves to a near stop hundreds of times a day, requiring additional energy to re-gain momentum and running the risk of losing agile prey from the mouth. This question will likely only be resolved by using direct speed measurements on lunge-feeding fin and blue whales. However, a key related issue that sheds light on how lunges are performed is the timing of the mouth opening and closure.

In an anatomical study of the jaw and ventral groove musculature in rorquals, Potvin et al. (Potvin et al., 2010) concluded that the jaws must open gradually during lunges to control the ingress of water into the buccal pouch. This is necessary to prevent the sudden parachute-like inflation of the cavity, which would create extreme stresses in the tissues. Such a powerful event should also produce a distinctive high-magnitude jerk signal, which would be easily detected above the cyclic signal from fluke movements, given the high sensor sampling rates used here. We see no massive initial jerk in the nearly 500 lunges analyzed. Instead, jerk increased steadily in each lunge (Fig. 4) as stroking movements became more forceful. Although we cannot exclude the possibility that the mouth opens synchronously with stroking, the lack of a distinct jerk signal supports the proposal of Potvin et al. (Potvin et al., 2010) that the jaw opening is a carefully controlled event. The accelerometers do, however, provide a strong clue as to when the jaws are open during

Table 3. Timing of events in lunges relative to zero-time defined by the falling half power point of flow noise

Lunge events re. zero-time in s	mn180a	mn192a	mn203a	mn155a	mn156a	Mean
Peak MSA	–1.16±0.87	–2.04±0.80	–1.81±0.55	–2.66±1.93	–2.12±1.98	–1.96±0.54
Peak flow noise	–0.67±0.65	–0.93±0.59	–0.98±0.42	–1.31±1.06	–1.91±1.09	–1.16±0.48
Peak depth rate	–1.19±1.31	–0.66±1.04	–1.30±0.56	–1.20±1.06	–1.77±1.45	–1.22±0.39
Last jerk peak	1.73±0.77	0.56±0.70	1.48±0.35	1.45±0.80	1.42±0.55	1.33±0.45
Peak of last upstroke	1.72±1.69	1.78±0.75	1.98±0.47	1.39±0.73	1.16±0.46	1.61±0.33

All times are the mean (±s.d.) in seconds over the lunges made by each animal.
MSA, minimum specific acceleration.

lunges. Both the stroking rate and the MSA, a lower bound on the net acceleration of the animal's body at the tag location, reach peak values during lunges that are much higher than during normal swimming in descents and ascents. Stroking rates were 50–100% faster whereas MSA, averaged over fluke strokes, was up to seven times greater. These robust peaks in MSA may provide a readily detectable lunge signal that could be counted by a tag enabling accurate long-term information about feeding behavior to be collected and transmitted *via* low-bandwidth satellite telemetry.

Despite the vigorous swimming, peak speeds within lunges, estimated using both fluke noise and depth rate, are only a little higher than those attained in the transport phases of dives (Fig. 6). This, in combination with the stronger and faster fluking in lunges, is a strong indication that the whales are working against a resistance much greater than the drag and buoyancy forces that oppose forward motion during descents and ascents. The implication is that the mouth must already be open and the buccal pouch inflated enough to create a higher drag when the high stroking rates and MSA occur within lunges. As the MSA reaches a peak an average of 2 s before the drop in flow noise (Table 3), we conclude that the mouth must begin opening a second or so before this and therefore some 3 s earlier than predicted by the lunge-stop model of Goldbogen et al. (Goldbogen et al., 2006). This conclusion is supported by Crittercam recordings of another lunging rorqual species, the blue whale, which show that the mouth opens before the flow noise begins to drop (Calambokidis et al., 2007).

Additional supporting data on the gape procession in lunges come from the stereotypy of stroking motions in the latter half of the lunge.

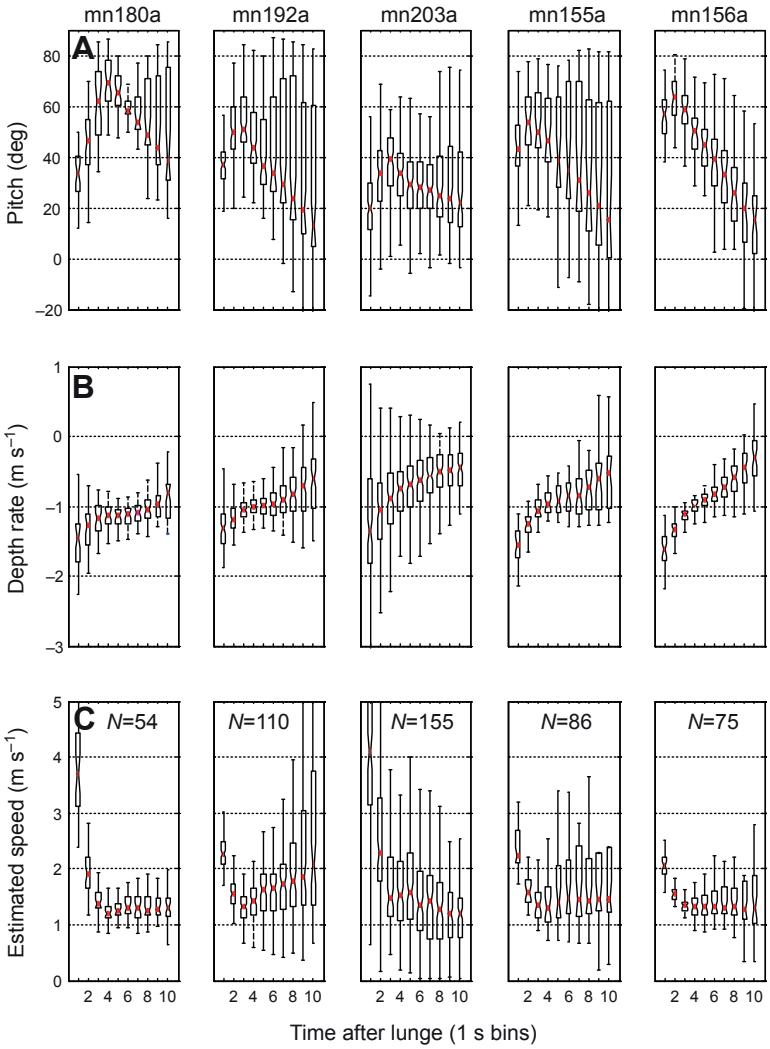

Fig. 6. Pitch and speed development in 1 s intervals within the 10 s after the lunge cue. (A) Mean pitch angle. (B) Depth rate. (C) Estimated forward speed (mean depth rate divided by the mean *x*-axis acceleration signal within each 1 s bin).

All five tagged animals timed their movements so as to begin the upstroke of a final slow fluke stroke when the sudden drop in flow noise occurs (Figs 3, 4). The slower stroking, and consequent lower MSA and jerk, after this point indicate the end of strong thrust production. As described by Potvin et al. (Potvin et al., 2010), considerable force is required to stretch the ventral groove blubber (VGB) that lines the lower margin of the buccal pouch and so maximize the volume of this cavity. Although the tongue may play a role, no other musculature is available to perform this task and so part of the force must be generated by the forward movement of the whale against the engulfed water, requiring a high speed [e.g. 3 m s^{-1} (Potvin et al., 2010)] to create the requisite pressure head. Given the high forces required, the VGB stretching must occur at the peak speed, i.e. before the drop in flow noise, taking advantage of the difference in speed between the animal and the water in the buccal cavity. Thus, one function of thrust production in the energetic phase of lunges is to transfer energy to the VGB. The energy stored in the elastic VGB material will later aid in emptying the buccal pouch when the stretching force is removed. As the VGB reaches the limit of its compliance, momentum begins to be transferred to the fluid in the buccal cavity. We suggest that this coincides with the end of vigorous stroking, with the subsequent sudden drop in speed indicating the final stage of momentum transfer to the engulfed water. Following this argument, the mouth should be closed rapidly when the forward speed drops to maintain the energy invested in the stretched VGB and to prevent fast reflux of water from the mouth driven by the contracting VGB. Mouth closure must then start around the moment of peak speed and continue through the subsequent distinctive speed drop. We suggest that the stereotypy of body motions at this point in the lunge indicates a change in activity from thrust production to gape closure with an upwards body rotation serving perhaps to move the engulfed water lower into the buccal pouch and facilitate jaw movement.

Data supporting our assertion regarding mouth closure come from the jerk signal. Jerk is the rate of change of acceleration and so emphasizes rapid body motions. Jerk transients are generated by stroking but can also be caused by any sudden muscle movement or collision of surfaces. Strong jerk signals were recorded throughout lunges on all tagged whales consistent with energetic stroking. But in whales with anterior tag placements, an additional jerk transient was recorded consistently at the end of lunges (Fig. 4H, green arrow). This transient occurs an average of 1.3 s after the speed drop, i.e. the zero-time of the lunge (Table 3), and does not seem to be connected with stroking motions, which are generally weak by this point. The jerk decays rapidly after the last transient and remains low until the beginning of the next lunge (Fig. 4). Given the timing of this final transient and its appearance in tags that are placed closer to the jaws, we suggest that it results from a tissue collision or muscle contraction at the end of mouth closure. Thus, we argue that mouth closure begins at the moment of peak speed, shortly before the drop in flow noise, and ends some 2.3 s later at the last jerk transient. By this point, the whale and the engulfed water are both moving forward at a steady speed of ~1–1.5 m s^{-1} and sieving of the trapped prey over the baleens can begin.

In the lunge-stop model of Goldbogen et al. (Goldbogen et al., 2006), the mouth opening coincides with, and causes, the sudden decrease in flow noise and hence inferred speed. We have presented evidence here that the mouth is open before the drop in speed, but perhaps as a result of the gradual gape opening, there is no clear acceleration signal that pinpoints when opening actually begins. Potvin et al. (Potvin et al., 2010) estimate a time period of 4 s from mouth opening to closure from videos of 10 humpback whales lunge feeding at the sea surface. However, these authors report difficulty in tracking the entire gape cycle in this footage and accept that their figure is an approximation. For our humpback whales lunging at >40 m depth, the gape cycle may be a little longer than this estimate. If the final jerk transient reflects mouth closure and the mouth opens before the peak in MSA, as we have argued, then a 5–6 s gape cycle is implied. Using this figure, we propose the following sequence of events in lunges: (1) whales stroke to increase speed in preparation for a lunge; (2) the mouth opens and two large fluke strokes are made to accelerate the whale against the water and so stretch the buccal cavity; (3) the mouth begins to close as the VGB reaches its limit of compliance and momentum is transferred to the engulfed water; and (4) speed drops rapidly as the water is accelerated and a final slower fluke stroke is made; the jaws close completely and the whale glides forwards and upwards with the engulfed water.

If this sequence is correct, it provides new insight into the forces and energetic costs in lunge feeding. To catch fast prey by lunge feeding, three things are necessary: large gape aperture, fast forward speed while approaching and surrounding the prey, and a large engulfment volume. These requirements are energetically costly, resulting in short dive times (Croll et al., 2001; Acevedo-Gutiérrez et al., 2002), but we suggest that the process provides a greater foraging efficiency than predicted by the current lunge-stop model. Goldbogen et al. (Goldbogen et al., 2007) predicted that drag from the open mouth was the main determinant of energetic cost in lunges. They combined a model for gape angle with the estimated speed reduction inferred from flow noise to estimate the drag force, finding a close correlation between gape angle and drag (Goldbogen et al., 2007; Potvin et al., 2009). However, a smooth gape angle curve starting at maximum speed and ending at minimum speed is bound to correlate closely with the differential of the speed curve to which it is matched and from which deceleration is derived [e.g. fig. 4 in Goldbogen et al. (Goldbogen et al., 2007)] and so this correlation may be trivial. Their model is aided by the long (~6 s) deceleration time recorded in blue whales, which fits well with the expected gape cycle duration. Higher-sampling-rate data from humpback whales presented here indicates a much shorter deceleration time (~1 s) for this species, far too short to encompass a gape cycle. An additional difficulty with the late-gape-opening model is that it requires stretching of the VGB and entrapment of prey to occur when the whale has already decelerated below 1.5 m s^{-1}, leaving much less force available for stretching and facilitating escape by mobile nektonic prey.

Our interpretation is that lunge-feeding humpbacks open their mouths earlier and use their peak speed to maximally fill the buccal pouch. In this model, whales engulf the water mass with one or two large fluke strokes and then decelerate as momentum is shared with an already fully stretched pouch of water and its trapped load of prey. This technique transfers energy from locomotion to the VGB tendons and to the engulfed water while minimizing acceleration of the surrounding fluid. Whales end lunges with some 1–1.5 m s^{-1} of forward speed, avoiding energy expenditure in re-starting from a halt as predicted in the previous lunge-stop model (Goldbogen et al., 2007). Taken together, these insights suggest that the success of lunge feeding as a foraging mode is a result of tight anatomical and behavioral integration, matched to the evasive behavior of the targeted nekton.

Filtering rate

Having engulfed a body mass of prey-laden water, tagged humpback whales exited most lunges gliding at ~1 m s^{-1} (Fig. 6). Exceptions to this were lunges made at the start of ascents, after which the

whales continued to fluke towards the surface. When multiple lunges were made in a dive, the inter-lunge intervals (ILIs) were reasonably constant within and across the five whales, suggesting that biomechanical limitations associated with harvesting prey from the engulfed water control the time between lunges. If the following lunge is initiated as soon as harvesting is complete, then filtering and ingestion require a mean of ~46 s (from mouth closure to the start of stroking in the next lunge; Table 2). Thus it seems that humpback whales spend approximately an order of magnitude longer to harvest prey from the water than they take to engulf it.

Assuming an engulfed water volume of 30 m^3 per lunge (Goldbogen et al., 2010) and a processing time of ~46 s, the mean filtering rate of a humpback whale may be ~0.7 $m^3 s^{-1}$. This is probably an underestimate as part of the ILI must be allocated to ingestion, but it is nonetheless approximately one-quarter of the ram filtration rate (3.2 $m^3 s^{-1}$) of the similarly sized bowhead whale (Simon et al., 2009). Integrated over a sequence of foraging dives, a bowhead whale filters approximately six times as much water as a humpback whale per unit of time foraging (Fig. 7). So why did rorquals such as humpback whales evolve an energetic and seemingly inefficient prey harvesting strategy as compared with balaenids? The answer is likely linked to the behavior of prey and the density of prey aggregations. Like other rorquals, humpback whales target fast-moving elusive nekton for which rapid engulfment is required, precluding the use of slow continuous ram filtration. The reported prey densities near feeding rorquals [0.01–0.5 kg m^{-3} (Sameoto, 1983; Piatt and Methven, 1992)] are 10-fold higher than copepod densities near ram-filtering balaenids [0.001–0.01 kg m^{-3} (Mayo and Goldman, 1992; Beardsley et al., 1996; Laidre et al., 2007)]. Although these estimates likely underestimate the actual prey densities encountered by whales (Laidre et al., 2007), the suggestion is that the lower filtering rate of rorquals is offset by denser prey patches. This may result in a similar energetic gain per unit of time for balaenids and rorquals despite their very different feeding strategies, which allows for niche segregation in highly productive areas.

Biomechanical and behavioral constraints

We have argued that lunges involve a strict sequence of biomechanical events, each of which creates a more-or-less distinct movement signature detectable with wide bandwidth accelerometer and pressure sensors (Figs 4, 5). To be effective in acquiring mobile prey, these movements must occur rapidly so that once a lunge has been initiated, the whale is likely bound to follow the sequence to its end. As pointed out by Ware et al. (Ware et al., 2011), the surprisingly stable ILIs across rorqual species suggest that the inter-lunge behaviors also seem to operate under biomechanical limitations that dictate when a new lunge is possible. We hypothesize that the minimum ILI is related to filtering rate, implying that the volume of water engulfed, which dictates the filtering time, is fairly constant: whales do not seem to scale the lunge according to patch size. Instead, rorquals lunging at depth seem to locate a food layer with density and size sufficient to support sequential lunges, and then perform these at a biomechanically limited rate. This is in contrast to other humpback feeding modes such as bubble-net feeding, in which prey are concentrated before a lunge (Jurasz and Jurasz, 1979; D'Vincent et al., 1985).

Given that most of the ILI is spent filtering and the objective of a rorqual is to lunge as often as possible, why did they not evolve faster filtration? One possibility is that this is dictated by the flow regime of water over the baleens to ensure effective filtration. Another may be that the number of lunges in a dive is limited anyway for energetic reasons. Goldbogen et al. (Goldbogen et al., 2010) reported maximum lunge counts per dive of six, eight and 15 for blue, fin and humpback whales, respectively, concluding that the increase in mass-specific expenditure with body size may explain the inverse relationship between lunge count and body mass (Goldbogen et al., 2012). However, with a maximum of four to nine lunges per dive, the humpback whales in the present study do not seem to fit this pattern. One explanation is that the number of lunges per dive relates to the quality of the food patch, with lower lunge counts in poorer food layers (Goldbogen et al., 2010). An alternative explanation relates to the behavior of prey. The humpback whales tagged in the Goldbogen et al. (Goldbogen et al., 2008) study were assumed to feed on krill whereas whales in the present study may be targeting fast and elusive schooling fish such as capelin (Kapel, 1979). To capture fast-moving prey, whales may have to accelerate more rapidly and so use more energy per lunge, limiting the number of lunges that can be performed in a dive. Presumably, whales feeding on such mobile prey gain from the greater nutritional value

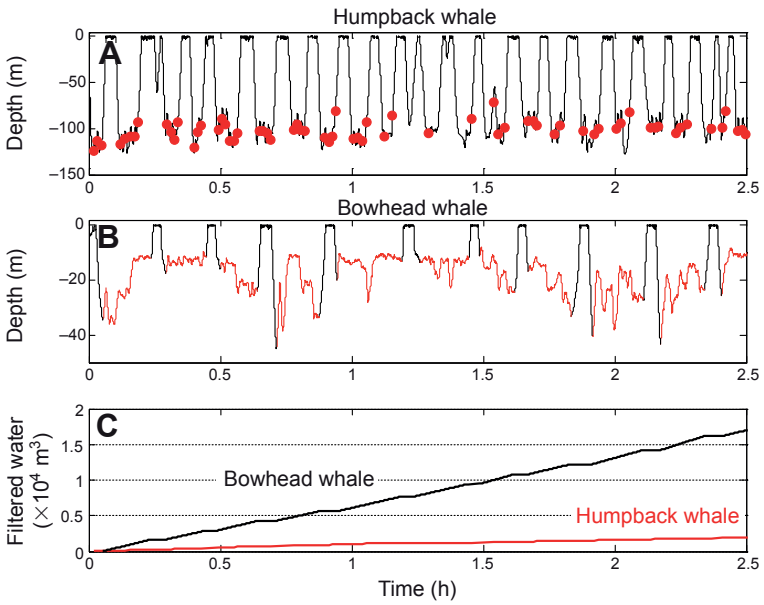

Fig. 7. Comparison of baleen whale foraging. (A) Dive profile of a humpback whale tagged with a DTAG in Nuuk fjord. The red circles indicate lunges detected by MSA. (B) Dive profile of a bowhead whale tagged with a DTAG in Disko Bay, Greenland (Simon et al., 2009). The red sections of the diving profile indicate feeding activity by ram filtration. (C) Estimated accumulated water filtered by a bowhead whale (black line) assuming a cross-sectional gape area of 4.23 m^2 (Werth, 2004) and a speed 0.75 m s^{-1} (Simon et al., 2009), and a humpback whale (red line) assuming an engulfment volume of 30 tons per lunge.

of these species despite the decreased volume of filtered water per unit time. However, given the challenges of *in situ* measurements of prey type and density around feeding whales, this conjecture remains to be tested.

Conclusions

Analysis of 479 lunges performed by humpback whales feeding at depth, tagged with fast-sampling multiple-sensor DTAGs, has provided detailed insights into the kinematics of rorqual lunge feeding. The consistency in the relative timing of accelerometer, flow noise and pressure signatures shows that lunge feeding is a highly stereotyped behavior tuned for efficient capture of small mobile prey. Prior observations of rorqual lunging with lower sensor sampling rates were interpreted as indicating that whales were brought to a near-standstill at the end of each lunge by drag from the open mouth, but this interpretation suffers from a number of biomechanical inconsistencies. Here we have shown that humpback whales accelerate as they acquire prey, opening their gape gradually in synchrony with strong fluke strokes. The forward speed during engulfment serves both to corral active prey and to expand the ventral margin of the buccal pouch and so maximize the engulfed water volume. Deceleration begins when the pouch nears full expansion and momentum starts to be transferred to the engulfed water. At the end of the lunge, the whales' momentum is shared with the load of water, leaving both whale and water gliding at ~1–1.5 m s^{-1}. Subsequent filtration takes some 46 s and is followed by stroking for the next lunge. Hence, lunge-feeding humpback whales do not come to a drag-induced halt, as previously proposed, but rather fluke throughout lunges, transferring energy to the engulfed water in a carefully orchestrated gape cycle that leaves whales with forward momentum at the end of each lunge. Despite this careful orchestration of biomechanical events, the high acceleration in lunges is energetically costly, but fast approaches are a prerequisite to capture the mobile and elusive nekton that rorquals have evolved to target. This is in contrast to the slow continuous ram filter-feeding strategy used by the related balaenid baleen whales, which capture much slower plankton. Nonetheless, the higher biomass densities in schools of nekton targeted by rorquals make this strategy rewarding. For future studies, the MSA and jerk signals derived from the fast-sampled three-axis accelerometers provide reliable cues for lunge feeding events, with prospects for on-board processing using satellite telemetry to reveal detailed behavioral and energy–time budgets of rorquals feeding over long time scales.

LIST OF SYMBOLS AND ABBREVIATIONS

A	total acceleration measured by the tag in three axes, $A=[a_x,a_y,a_z]^T$; axes x, y and z are defined as the caudal–rostral, ventral–dorsal and left–right, respectively
D	specific acceleration vector
T	sensor sampling interval (s)
$\boldsymbol{g}$	acceleration due to gravity (9.81 m s^{-2})
G	gravitational acceleration vector ($\boldsymbol{g}$); $\mathbf{G}=[0,0,1]^T$ in a {north,west,down} coordinate system.
MSA	minimum specific acceleration (m s^{-2})
Q_t	direction cosine matrix describing the instantaneous orientation of the whale with respect to the inertial frame
t	time (s)

ACKNOWLEDGEMENTS

We thank T. Boye, F. Ugarte, B. K. Nielsen, M. Møller, L. Heilman and S. Perez for help in the field; T. Hurst for tag preparation; and J. A. Goldbogen, A. Werth, F. Ugarte, B. Wursig, P. Tyack and two anonymous reviewers for helpful discussions or comments on previous versions of the manuscript.

FUNDING

M.S. was funded by the Oticon Foundation and Ministry of Education, Research and Nordic Cooperation, Greenland Government, Greenland Self Government. P.T.M. was funded by Steno and frame grants from the National Danish Science Foundation. M.J. was funded by National Ocean Partnership Program (NOPP) and Strategic Environmental Research and Development Program (SERDP) grants.

REFERENCES

Acevedo-Gutiérrez, A., Croll, D. A. and Tershy, B. R. (2002). High feeding costs limit dive time in the largest whales. *J. Exp. Biol.* **205**, 1747-1753.

Beardsley, R., Epstein, A. W., Chen, C., Wishner, K. F., Macaulay, M. C. and Kenney, R. D. (1996). Spatial variability in zooplankton abundance near feeding right whales in the Great South Channel. *Deep Sea Res. Part II Top. Stud. Oceanogr.* **43**, 1601-1625.

Blackwell, S. B., Haverl, C. A., Le Boeuf, B. J. and Costa, D. P. (1999). A method for calibrating swim-speed recorders. *Mar. Mamm. Sci.* **15**, 894-905.

Brodie, P. F. (1993). Noise generated by the jaw actions of feeding fin whales. *Can. Zool.* **71**, 2546-2550.

Burgess, W. C., Tyack, P. L., Le Boeuf, B. J. and Costa, D. P. (1998). A programmable acoustic recording tag and first results from free-ranging northern elephant seals. *Deep-Sea Res.* **45**, 1327-1351.

Calambokidis, J., Schorr, G. S., Steiger, G. H., Francis, J., Bakhtiari, M., Marshall, G., Oleson, E. M., Gendron, D. and Robertson, K. (2007). Insights into the underwater diving, feeding, and calling behavior of blue whales from a suction-cup-attached video-imaging tag (Crittercam). *Mar. Technol. Soc. J.* **41**, 19-29.

Cooper, L. N., Sedano, N., Johansson, S., May, B., Brown, J. D., Holliday, C. M., Kot, B. W. and Fish, F. E. (2008). Hydrodynamic performance of the minke whale (*Balaenoptera acutorostrata*) flipper. *J. Exp. Biol.* **211**, 1859-1867.

Croll, D. A. and Tershy, B. (2002). Filter feeding. In *Encyclopedia of Marine Mammals* (ed. W. F. Perrin, B. Würsig, B. and J. G. M. Thewissen), pp. 428-432. London: Academic Press.

Croll, D. A., Acevedo-Gutiérrez, A., Tershy, B. R. and Urbán-Ramírez, J. (2001). The diving behavior of blue and fin whales: is dive duration shorter than expected based on oxygen stores? *Comp. Biochem. Physiol.* **129A**, 797-809.

D'Vincent, C. G., Nilson, R. M. and Hanna, R. E. (1985). Vocalization and coordinated feeding behavior of the humpback whale in southeastern Alaska. *Sci. Rep. Whales Res. Inst.* **36**, 41-47.

Doniol-Valcroze, T., Lesage, V., Giard, J. and Michaud, R. (2011). Optimal foraging theory predicts diving and feeding strategies of the largest marine predators. *Behav. Ecol.* **22**, 880-888.

Fish, F. E., Peacock, J. E. and Rohr, J. J. (2003). Stabilization mechanism in swimming odontocete cetaceans by phased movements. *Mar. Mamm. Sci.* **19**, 515-528.

Fish, F. E., Howle, L. E. and Murray, M. M. (2008). Hydrodynamic flow control in marine mammals. *Integr. Comp. Biol.* **48**, 788-800.

Goldbogen, J. A., Calambokidis, J., Shadwick, R. E., Oleson, E. M., McDonald, M. A. and Hildebrand, J. A. (2006). Kinematics of foraging dives and lunge-feeding in fin whales. *J. Exp. Biol.* **209**, 1231-1244.

Goldbogen, J. A., Pyenson, N. D. and Shadwick, R. E. (2007). Big gulps require high drag for fin whale lunge feeding. *Mar. Ecol. Prog. Ser.* **349**, 289-301.

Goldbogen, J. A., Calambokidis, J., Croll, D. A., Harvey, J. T., Newton, K. M., Oleson, E. M., Schorr, G. and Shadwick, R. E. (2008). Foraging behavior of humpback whales: kinematic and respiratory patterns suggest a high cost for a lunge. *J. Exp. Biol.* **211**, 3712-3719.

Goldbogen, J. A., Potvin, J. and Shadwick, R. E. (2010). Skull and buccal cavity allometry increase mass-specific engulfment capacity in fin whales. *Proc. Biol. Sci.* **2010**, 861-868.

Goldbogen, J. A., Calambokidis, J., Oleson, E. M., Potvin, J., Pyenson, N. D., Schorr, G. and Shadwick, R. E. (2011). Mechanics, hydrodynamics and energetics of blue whale lunge feeding: efficiency dependence on krill density. *J. Exp. Biol.* **214**, 131-146.

Goldbogen, J. A., Calambokidis, J., Croll, D. A., McKenna, M. F., Oleson, E., Potvin, J., Pyenson, N. D., Schorr, G., Shadwick, R. E. and Tershy, B. R. (2012). Scaling of lunge-feeding performance in rorqual whales: mass-specific energy expenditure increases with body size and progressively limits diving capacity. *Funct. Ecol.* **26**, 216-226.

Golub, G. and Loan, V. (1996). Matrix analysis. In *Matrix Computations* (ed. J. Hopkins), pp. 48-86. Lanham-Seabrook, MD: University Press.

Grewal, M. and Weill, L. R. and Andrews, A. P. (2001). *Global Positioning Systems, Inertial Navigation, and Integration*. New York: John Wiley & Sons.

Hochachka, P. W. and Somero, G. N. (1984). *Biochemical Adaptation*. Princeton, NJ: Princeton University Press.

Johnson, M., Aguilar Soto, N. and Madsen, P. T. (2009). Studying the behaviour and sensory ecology of marine mammals using acoustic recording tags: a review. *Mar. Ecol. Prog. Ser.* **395**, 55-73.

Johnson, M. P. and Tyack, P. L. (2003). A digital acoustic recording tag for measureing the response of wild marine mammals to sound. *IEEE J. Oceanogr. Eng.* **28**, 3-12.

Jurasz, C. M. and Jurasz, V. P. (1979). Feeding modes of the humpback whales, *Megaptera novaeangliae*, in southeast Alaska. *Sci. Rep. Whales Res. Inst.* **31**, 69-83.

Kapel, F. O. (1979). Exploitation of large whales in west Greenland in the twentieth Century. *Rep. Int. Whaling Comm.* **29**, 197-214.

Kooyman, G. L. (1989). *Diverse Divers: Physiology and Behavior*. Berlin: Springer-Verlag.

Kooyman, G. L., Wahrenbrock, E. A., Castellini, M. A., Davis, R. A. and Sinnett, E. E. (1980). Aerobic and anaerobic metabolism during diving in Weddell seals: evidence of preferred pathways from blood chemistry and behavior. *J. Comp. Physiol.* **138**, 335-346.

Kramer, D. L. (1988). The behavioural ecology of air breathing by aquatic animals. *Can. J. Zool.* **66**, 89-94.
Laidre, K. L., Heide-Jørgensen, M. P. and Nielsen, T. G. (2007). Role of the bowhead whale as a predator in West Greenland. *Mar. Ecol. Prog. Ser.* **346**, 285-297.
Lambertsen, R. H. (1983). Internal mechanism of rorqual feeding. *J. Mammal.* **64**, 76-88.
Mayo, C. A. and Goldman, L. (1992). Right whale foraging and the plankton resources in Cape Cod and Massachusetts Bays. In *The Right Whale in the Western North Atlantic: A Science and Management Workshop* (ed. J. Hain), pp. 43-44. Northeast Fisheries Science Center Ref. Doc. 92-05.
Miller, P. J. O., Johnson, M. P., Tyack, P. L. and Terray, E. A. (2004). Swimming gaits, passive drag and buoyancy of diving sperm whales *Physeter macrocephalus*. *J. Exp. Biol.* **207**, 1953-1967.
Moore, M. J., Miller, C. A., Morss, M. S., Arthur, R., Lange, W., Prada, K. G., Marx, M. K. and Frey, E. A. (2001). Ultrasonic measurement of blubber thickness in right whales. *J. Cetacean Res. Manag.* **2**, 301-309.
Nowacek, D. P., Johnson, M. P. and Tyack, P. L. (2004). North Atlantic right whales (*Eubalaena glacialis*) ignore ships but respond to alerting stimuli. *Proc. Biol. Sci.* **271**, 227-231.
Orton, L. S. and Brodie, P. F. (1987). Engulfing mechanics of fin whales. *Can. J. Zool.* **65**, 2898-2907.
Piatt, J. F. and Methven, D. A. (1992). Threshold foraging behavior of baleen whales. *Mar. Ecol. Prog. Ser.* **84**, 205-210.
Pivorunas, A. (1979). The feeding mechanisms of baleen whales. *Am. Sci.* **67**, 432-440.
Potvin, J., Goldbogen, J. A. and Shadwick, R. E. (2009). Passive versus active engulfment: verdict from trajectory simulations of lunge-feeding fin whales *Balaenoptera physalus*. *J. R. Soc. Interface* **6**, 1005-1025.
Potvin, J., Goldbogen, J. A. and Shadwick, R. E. (2010). Scaling of lunge feeding in rorqual whales: an integrated model of engulfment duration. *J. Theor. Biol.* **267**, 437-453.
Sameoto, D. D. (1983). Euphausiid distribution in acoustic scattering layers and its significance to surface swarms. *J. Plankton Res.* **5**, 129-143.
Sato, K., Watanuki, Y., Takahashi, A., Miller, P. J., Tanaka, H., Kawabe, R., Ponganis, P. J., Handrich, Y., Akamatsu, T., Watanabe, Y. et al. (2007). Stroke frequency, but not swimming speed, is related to body size in free-ranging seabirds, pinnipeds and cetaceans. *Proc. R. Soc. B* **274**, 471-477.
Shepard, E. L. C., Wilson, R. P., Liebsch, N., Quintana, F., Laich, A. G. and Lucke, K. (2008). Flexible paddle sheds new light on speed: a novel method for the remote measurement of swim speed in aquatic animals. *Endanger. Species Res.* **4**, 157-164.
Simon, M., Johnson, M., Tyack, P. and Madsen, P. T. (2009). Behaviour and kinematics of continuous ram filtration in bowhead whales (*Balaena mysticetus*). *Proc. Biol. Sci.* **276**, 3819-3828.
Ware, C., Friedlander, A. S. and Nowacek, D. P. (2011). Shallow and deep lunge feeding of humpback whales in fjords of the West Antarctic Peninsula. *Mar. Mamm. Sci.* **27**, 587-605.
Watanuki, Y., Niizuma, Y., Gabrielsen, G. W., Sato, K. and Naito, Y. (2003). Stroke and glide of wing-propelled divers: deep diving seabirds adjust surge frequency to buoyancy change with depth. *Proc. Biol. Sci.* **270**, 483-488.
Watkins, W. A. and Schevill, W. E. (1979). Aerial observations of feeding behavior in four baleen whales: *Eubalaena glacialis*, *Balaenoptera borealis*, *Megaptera novaeangliae*, and *Balaenoptera physalus*. *J. Mammal.* **60**, 155-163.
Werth, A. J. (2000). Marine Mammals. In *Feeding: Form, Function and Evolution in Tetrapos Vertebrates* (ed. K. Schwenk), pp. 475-514. New York: Academic Press.
Werth, A. J. (2004). Models of hydrodynamic flow in the bowhead whale filter feeding apparatus. *J. Exp. Biol.* **207**, 3569-3580.
Williams, T. M., Davis, R. W., Fuiman, L. A., Francis, J., Le Boeuf, B. J., Horning, M., Calambokidis, J. and Croll, D. A. (2000). Sink or swim: strategies for cost-efficient diving by marine mammals. *Science* **288**, 133-136.
Zimmer, W. M., Johnson, M. P., Madsen, P. T. and Tyack, P. L. (2005). Echolocation clicks of free-ranging Cuvier's beaked whales (*Ziphius cavirostris*). *J. Acoust. Soc. Am.* **117**, 3919-3927.